

pubs.acs.org/JPCB Article

Ligand-Dependent Volumetric Characterization of Manganese Riboswitch Folding: A High-Pressure Single-Molecule Kinetic Study

Hsuan-Lei Sung and David J. Nesbitt*



Cite This: J. Phys. Chem. B 2022, 126, 9781-9789



ACCESS

Metrics & More

Priboswitch unfolds

pressure increase

Priboswitch unfolds

priboswitch unfolds

priboswitch unfolds

priboswitch unfolds

priboswitch unfolds

ABSTRACT: Nanoscopic differences in free volume result in pressure-dependent changes in free energies which can therefore impact folding/unfolding stability of biomolecules. Although such effects are typically insignificant under ambient pressure conditions, they are crucially important for deep ocean marine life, where the hydraulic pressure can be on the kilobar scale. In this work, single molecule FRET spectroscopy is used to study the effects of pressure on both the kinetics and overall thermodynamics for folding/unfolding of the manganese riboswitch. Detailed pressure-dependent analysis of the conformational kinetics allows one to extract precision changes ($\sigma \lesssim 4-8$ ų) in free volumes not only between the fully folded/unfolded conformations but also with respect to the folding transition state of the manganese riboswitch. This permits first extraction of a novel "reversible work" free energy ($P\Delta V$) landscape, which reveals a monotonic increase in manganese riboswitch volume along the folding coordinate. Furthermore, such a tool permits exploration of pressure-dependent effects on both Mn²+ binding and riboswitch folding, which demonstrate that ligand attachment stabilizes the riboswitch under pressure by decreasing the volume increase upon folding ($\Delta \Delta V < 0$). Such competition between ligand binding and pressure-induced denaturation dynamics could be of significant evolutionary advantage, compensating for a weakening in riboswitch tertiary structure with pressure-mediated ligand binding and promotion of folding response.

capillary cell

I. INTRODUCTION

Structural transitions in biomolecules and the associated reorganization of the surrounding water molecules lead to nanoscopic changes in the overall solvent plus solute system volume. As a result, conformational change in a biomolecule is intrinsically pressure-dependent. Though such pressure effects are often negligible at ambient pressure (1 bar), these effects can become quite significant in marine biology due to rapid increase in hydraulic pressure as a function of ocean depth (0.1 bar/m). Indeed, the average ocean depth already corresponds to 350 bar pressure, with the deepest regions (e.g., the Challenger Deep) in excess of 1 kbar. As a result, marine (micro)organisms can exhibit unique modes of biological function sculpted by evolution under high-pressure conditions. It is therefore of particular biophysical interest to explore pressure-dependent paradigms of biomolecular struc-

ture and function to understand, at the molecular level, bioadaptation of deep-sea organisms to pressure extremes.⁷

pressure (bar)

With a few exceptions, ^{8,9} proteins and nucleic acids are known to thermodynamically unfold/dehybridize with increasing pressure. ^{5,10–12} Pressure-induced denaturation implies that the folded solute + solvent system effectively occupies more space, resulting in a positive free volume change ($\Delta V^0 > 0$) upon folding. Such an increase in volume may seem initially counterintuitive because one often thinks of biomolecular

Received: September 14, 2022 Revised: October 21, 2022 Published: November 18, 2022





folding tending toward a state of greater compaction. One reason for such anomalous behavior is that these overall volume changes are quite modest, with solvent-excluding voids^{13–15} and/or reorganization of the solvation shell^{16–18} thought to be major contributors to the volume increase upon folding. Interestingly, although pressure is known to thermodynamically destabilize the equilibrium folding behavior for nucleic acids and proteins, the kinetics of such effects has remained far less explored.^{19–21} Furthermore, because nucleic acids conformations are often highly dynamic,²² with important biochemical pathways regulated by kinetic access over a barrier to a functionally new conformation (e.g., regulation of gene expression by co-transcriptional folding of riboswitches),^{23–25} it is therefore of particular importance to also explore the effects of pressure on *transition state barriers* and the resulting folding kinetics.

Recently, high-pressure single-molecule fluorescence resonance energy transfer (smFRET) studies of nucleic acid folding kinetics have become experimentally accessible, exploiting small glass capillaries as high-pressure sample cells in conjunction with confocal single photon counting fluorescence measurements. ^{11,26,27} In earlier work, pulsed laser excitation through a microscope objective into solutions at high pressure have been used to measure and record the FRET energy transfer efficiency (E_{FRET}) for single RNA molecules diffusing through the confocal volume region. Though such studies have been limited to equilibrium thermodynamics, they clearly demonstrated a systematic decrease in E_{FRET} (i.e., an increase in the unfolding fraction) with increasing pressure. In the present work, we significantly expand these equilibrium high-pressure smFRET studies by immobilizing single RNA constructs to the inside of a highpressure capillary cell and thereby extend observation times of the fluorescence trajectories to monitor folding/unfolding kinetics at the single molecule level.²⁸ The resulting pressuredependent kinetic rate constant data now inform on the free volume changes associated with (i) folded, (ii) unfolded, and (iii) transition state barrier conformations and thus provide novel opportunities for detailed characterization of the thermodynamic free volume along the nucleic acid folding coordinate.²⁹

Specifically, this work comprises detailed study of the effects of high pressure on the folding/unfolding kinetics of the manganese riboswitch at the single molecule level. The folding thermodynamics and kinetics of this riboswitch have been studied previously both in ensemble and at the single molecule level under ambient pressure (1 bar) conditions, 30-33 with the present work exploring pressure-dependent kinetics of ligandinduced tertiary structure formation for the first time. Of particular significance is first experimental characterization of the coupling between (i) pressure-dependent kinetic measurements and (ii) the ligand binding event, which allows us to obtain free volume changes for accessing the transition state associated with manganese riboswitch folding. Furthermore, in the context of a simple Hill analysis, 30 we can separate ligand Mn²⁺ binding from riboswitch folding events and thereby obtain novel information about "reversible work" $(P\Delta V)$ contributions to the free energy landscape along the conformational reaction path. These volume changes are revealed to be sensitive to the hydration structure and fractional Mn²⁺ binding with the RNA, which offers additional insights into the mechanism for ligand-induced RNA folding.

The organization of this paper is as follows. The details of sample preparation and high-pressure experiment setup are illustrated in Section II. Section IIIA demonstrates highpressure effects on the riboswitch folding kinetics, for which increasing pressure destabilizes the riboswitch by simultaneously decreasing (increasing) the folding (unfolding) rate constants. The effects of Mn2+ and Mg2+ cations on the pressure-dependent folding are then presented in Sections IIIB and IIIC, respectively, which reveal that cognate ligand Mn²⁺ (and not Mg2+) significantly impacts changes in free volume $(\Delta V_{\rm bind}^0 < 0)$. Specifically, Mn²⁺ alters the volumetric reversible work landscape for folding via binding of the cognate ligand to (and subsequent compaction of) the riboswitch rather than a more generic screening of anionic repulsion due to divalent cations. Finally, we briefly discuss in Sections IVA and IVB the possible role of equilibrium vs kinetic competition between Mn2+ and pressure-induced changes in riboswitch volume on the evolutionary biology of deep-sea organisms.

II. EXPERIMENT

IIA. Single-Molecule Fluorescent Construct Design and Sample Preparation. From the crystal structure data (PDB: 4Y11),³³ the ligand-bound folded conformation of the manganese riboswitch consists of an RNA four-way junction with the loop—loop interaction between P1 and P3 stems stabilized by a Mn²⁺ cation (Figure 1A). In design of the

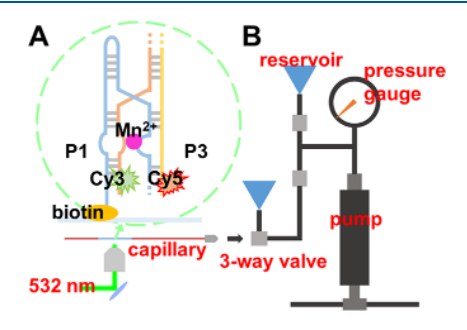


Figure 1. Schematic of the high-pressure single-molecule FRET experiment showing the instrument setup. (A) Cartoon representation of the manganese riboswitch construct in the Mn²⁺-bound folded conformation where the loop—loop interaction between P1 and P3 stems is formed. (B) High-pressure generating system coupling to the capillary sample holder aligned with the microscope objective. The reservoirs contain ethanol as the pressure transmitting fluid throughout the high-pressure tubing manifold.

single-molecule FRET construct, the manganese riboswitch is labeled with Cy3 and Cy5 at the distal ends of P1 and P3, respectively, to probe the loop—loop docking/undocking that is the major conformational response to Mn²+ association. The single-molecule FRET construct of the riboswitch consists of three RNA oligomers, labeled with Cy3, Cy5, and biotin. The detailed RNA sequences and the labeling positions for these oligomers can be found in previous work.³⁴ To assemble the ternary RNA construct, the three oligomers are heat-annealed at 90 °C, followed by purification via high-performance liquid chromatography (HPLC) methods. The doubly dye-labeled and biotinylated product enables surface immobilization of the RNA construct to achieve single-molecule fluorescence detection over a prolonged time window and thereby observe a sequence of multiple folding/unfolding events. Furthermore,

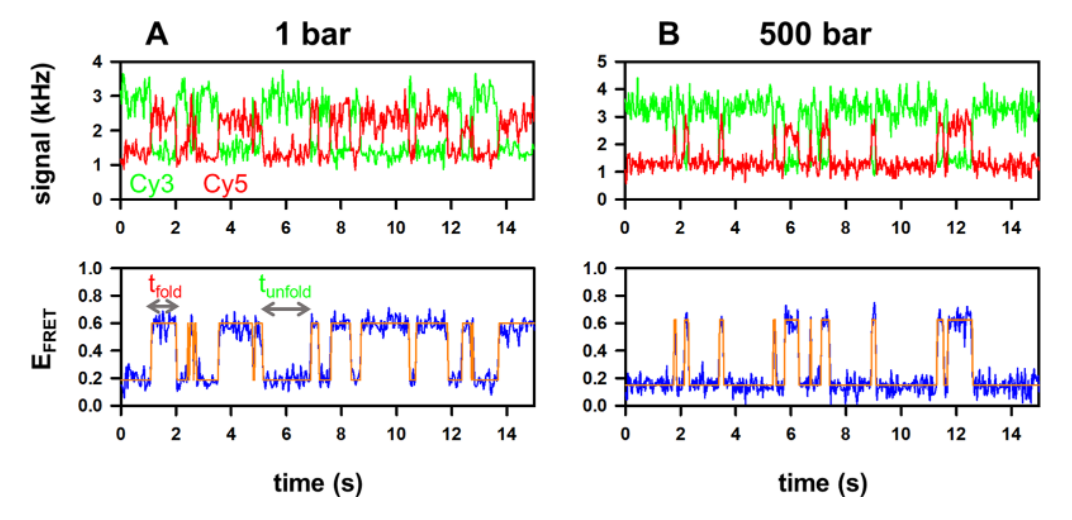


Figure 2. Sample fluorescence traces and the resulting time trajectories of E_{FRET} at (A) 1 bar and (B) 500 bar. The simulated traces in orange are obtained from hidden Markov modeling.

on the basis of a characteristic Forster length $R_0 \approx 50$ Å for the Cy3–Cy5 FRET pair, the interdye distances in the folded conformation can be predicted from the manganese riboswitch crystal structure to be 45 Å, which is in good agreement ($E_{\rm FRET}$ (45 Å) ≈ 0.65) with the high $E_{\rm FRET} \approx 0.60$ state observed. Conversely, when the manganese riboswitch unfolds, the distance between Cy3 and Cy5 increases, resulting in a reduced and easily distinguished value of $E_{\rm FRET} \approx 0.15$ consistent with $R \geq 67$ Å.

The high-pressure sample cell is made from a glass capillary with a square cross section (75 μ m/360 μ m inner/outer dimensions, Polymicro).²⁷ Such small lateral dimensions permit higher pressure (>2000 bar) operation, while the flat interior surface and wall thickness (143 μ m) also allow the capillary to function as a conventional coverslip in standard microscope imaging. To prepare the sample, one end of the capillary is first glued into a metal plug drilled with a 450 μ m diameter hole and coupled to the pressure system (Figure 1B). After creating an optically transparent window by oxidizing away a small 1 cm patch of the polymer coating, we immobilize the RNA molecules on the inner surface of the capillary through biotin-streptavidin interactions. To achieve this goal, we continuously flow the following solutions through the capillary in succession: (1) 10 mg/mL bovine serum albumin (BSA) with 10% biotinylation, (2) 200 μ g/mL streptavidin solution, and (3) ≈25 pM RNA construct. The exposure time for each solution is ≈2 min, with pressure delivered through a mechanical micropipet (Eppendorf) to flush liquid through the capillary.²⁹ Before any single molecule experiments, the capillary is additionally flushed with an imaging buffer containing (1) 50 mM pH 7.5 HEPES buffer, (2) enzymatic oxygen scavenger cocktail (PCD/PCA/Trolox) to catalytically remove oxygen, 35 (3) 100 mM NaCl to provide background salt, and (4) sufficient MgCl₂/MnCl₂ to achieve desired divalent cation and cognate ligand concentrations. The free end of the capillary is then sealed with an oxy-propane torch, while the metal plug end is dipped into silicon oil to create a thin pressure transmitting meniscus and prevent sample contamination.

IIB. High-Pressure Single-Molecule FRET Spectroscopy. Pressure control is achieved by a manually operated piston screw pump (High Pressure Equipment), which can deliver pressures up to 5 kbar through high-pressure stainless steel

tubing, with the entire manifold filled with ethanol as pressure transmitting fluid (Figure 1B).³⁶ We take advantage of the square cross section of the sample cell by taping it onto the surface of a coverslip, which permits ready alignment of the optical axis of the microscope objective axis with respect to the capillary wall.²⁹ The details of the confocal single molecule FRET spectroscopy setup can be found in previous work.³⁷ To initiate an experiment, the laser is focused to a diffraction limited waist ($\omega_{x,y} \approx 260 \ \mu \text{m}$) on the inner capillary surface, with the search for single fluorescent molecule constructs conducted by raster scanning of the piezo stage. Tethering of the construct to the capillary surface permits prolonged diffraction limited observation of Cy3/Cy5 fluorescence from a single localized RNA, which in turn enables the collection of long-lived (≈1 min) single molecule FRET trajectories at ≈4 kHz photon/s detection rates and limited by eventual photobleaching.

III. RESULTS AND ANALYSIS

IIIA. Kinetic Origins of Manganese Riboswitch Unfolding at Increasing Pressure. Time-dependent E_{FRET} trajectories reveal that the manganese riboswitch actively switches between low and high E_{FRET} states (see sample FRET traces in Figure 2) corresponding to unfolded and folded conformations.³⁰ While the equilibrium constant K_{fold} can be readily obtained from the total timing for folded vs unfolded events, even more valuable information about the folding kinetics can be extracted from the distribution of dwell times. As shown in Figure 3, this dwell time distribution is well approximated by a single-exponential decay, for which the folding/unfolding kinetics of the manganese riboswitch can be described by first-order rate constants $k_{\rm fold}$ and $k_{\rm unfold}$. The resulting dwell time analysis reveals a faster decay for the dwell time distribution of the unfolded state, i.e., $k_{\text{fold}} > k_{\text{unfold}}$ under ambient (1 bar) conditions. As external hydrostatic pressure increases to 500 bar, however, the riboswitch spends significantly longer in the low E_{FRET} ("denatured") conformation, as visually evident in Figure 2. Such pressuredependent denaturation is consistent with previous highpressure studies of both proteins^{5,12} and nucleic acids.¹ Interestingly, however, the dwell time distributions in Figure 3 make evident that increasing pressure kinetically results in an equilibrium preference for the unfolded Mn²⁺ riboswitch by

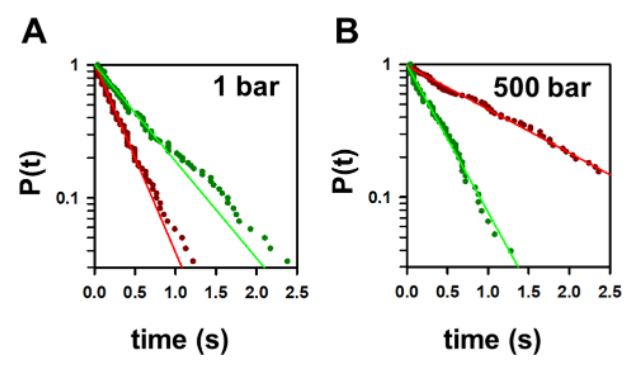


Figure 3. Sample dwell time distributions in semilogarithmic plots at (A) 1 bar and (B) 500 bar. Data are fit to a single-exponential decay function to obtain folding and unfolding rate constants $k_{\rm fold}$ and $k_{\rm unfold}$, respectively.

both an increase in the unfolding rate constant (k_{unfold}) and yet also a simultaneous decrease in the folding rate constant (k_{fold}).

The pressure effects on the manganese riboswitch folding equilibria can be summarized in the semilogarithm "van't Hoff" plots of K_{fold} vs pressure (Figure 4A), which specifically reveal

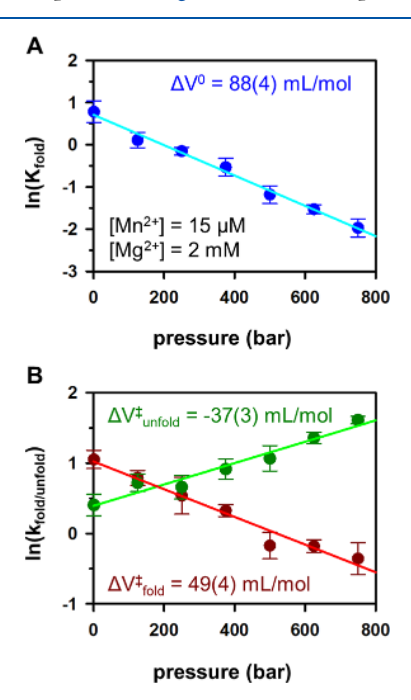


Figure 4. Pressure-dependent manganese riboswitch folding (A) equilibrium constant and (B) kinetics rate constant plots, where error bars represent standard deviation of the mean. In analogy to Eyring analysis of transition state barrier energies, the data are least-squares fit to a single-exponential function to obtain quantitative volumetric change information for ΔV^0 and $\Delta V^{\dagger}_{\text{fold/unfold}}$. [Mn²⁺] = 15 μ M; [Mg²⁺] = 2 mM.

a linear decrease in $\ln(K_{\rm fold})$ as a function of elevated pressure. We can further quantify such a pressure dependence by the simple thermodynamic relation^{3,5}

$$\left(\frac{\partial \ln K_{\rm fold}}{\partial P}\right)_T = \frac{-\Delta V^0}{RT} \tag{1}$$

which allows us to relate the slope in Figure 4A to the change in free volume upon folding. Least-squares fits to the data yield

 $\Delta V^0 = +88(4)$ mL/mol, with a positive sign clearly corresponding to the manganese riboswitch occupying the greater volume upon folding. The present high-pressure single-molecule kinetic capabilities permit a further interesting level of detail by similar volumetric analysis applied to pressure-dependence of the folding/unfolding rate constants (Figure 4B). Specifically, the activation free volume $\Delta V^{\ddagger}_{\text{fold/unfold}}$ for accessing the transition state barrier from the folded/unfolded conformations can be obtained from linear fits to an "Arrhenius-like" volumetric expression⁵

$$\left(\frac{\partial \ln k_{\text{fold/unfold}}}{\partial P}\right)_{T} = \frac{-\Delta V_{\text{fold/unfold}}^{\ddagger}}{RT} \tag{2}$$

where once again a positive volume change ($\Delta V^{\ddagger}_{\rm fold} = 49(4)$ mL/mol) reveals that the transition state (TS) takes up more volume than the fully unfolded state (U). Conversely, the corresponding volume change in the unfolding direction is negative ($\Delta V^{\ddagger}_{\rm unfold} = -37(3)$ mL/mol), which obviously rationalizes the observed speed up in the unfolding rate constant $k_{\rm unfold}$ with pressure. These results can be simply summarized as predicting a monotonic increase in the manganese riboswitch free volume along the folding coordinate, with $V_{\rm U} < V_{\rm TS} < V_{\rm F}$, with uncertainties in these volume changes at the $\sigma \lesssim 4-8$ Å 3 level.

Folding. The manganese riboswitch responds conformationally to its cognate ligand Mn²⁺ in the regulation of gene expression, which naturally invites study of pressure-dependent folding as a function of ligand concentration.³² As evident in Figure 5, increasing the cognate ligand Mn²⁺ concentration

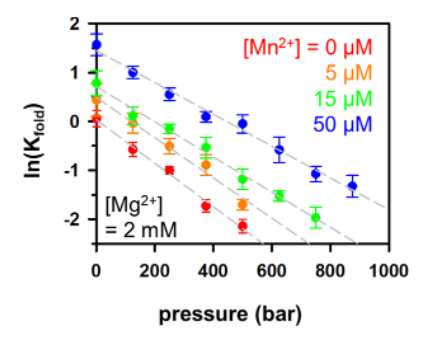


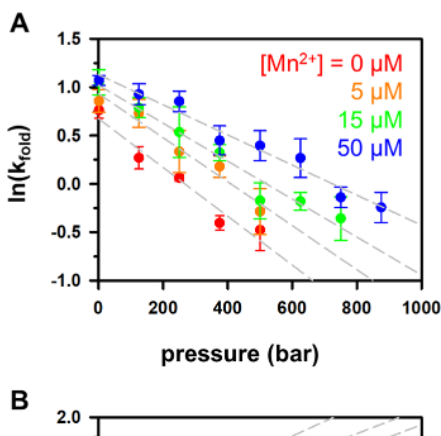
Figure 5. Pressure-dependent equilibrium constants (K_{fold}) for the riboswitch folding as a function of increasing [Mn²⁺] in the presence of physiological [Mg²⁺] = 2 mM.

promotes riboswitch folding (i.e., an increase in $K_{\rm eq}$) at each pressure explored from ambient to 1000 bar. Moreover, the slopes of the van't Hoff plots are all negative ($\Delta V^0 > 0$), correctly predicting pressure-induced denaturation for the manganese riboswitch at all Mn2+ concentrations within a physiologically relevant range. At a higher level of quantification, the van't Hoff slopes in Figure 5 are summarized in Table 1, for which the ΔV^0 values exhibit a systematic decrease as a function of increasing Mn2+. Most importantly, this implies that all positive free volume changes for manganese riboswitch folding/unfolding are significantly reduced by association with the cognate ligand/Mn²⁺, a point to which we will return in Section IV. Finally, we can apply a similar pressure- and Mn²⁺dependent analysis to the rate constants for manganese riboswitch folding/unfolding. As nicely summarized in Figures 6A,B, an increase in Mn²⁺ concentration systematically lowers

Table 1. ΔV^0 and $\Delta V^{\ddagger}_{\rm fold/unfold}$ Values as a Function of Increasing Mn^{2+ a}

$[\mathrm{Mn}^{2+}]/\Delta V \ (\mu\mathrm{M})$	$rac{\Delta V^0}{(ext{mL/mol})}$	$rac{\Delta V^{\ddagger}_{ m fold}}{({ m mL/mol})}$	$rac{\Delta V^{\ddagger}_{ m unfold}}{({ m mL/mol})}$
0	110 (4)	61(7)	-44(4)
5	100(7	56(7)	-39(4)
15	88(4)	49(4)	-37(3)
50	79(3)	38(2)	-41(3)

^aThe reported uncertainties represent standard deviation of the mean for triplicate studies.



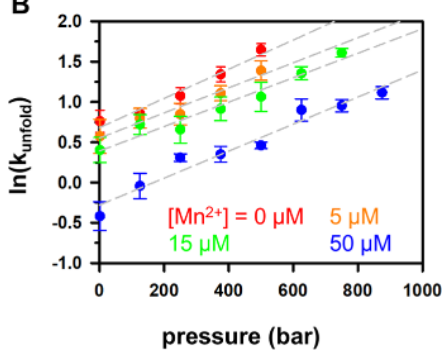


Figure 6. Pressure-dependent rate constants (A) k_{fold} and (B) k_{unfold} as a function of increasing [Mn²⁺] in the presence of physiological [Mg²⁺] = 2 mM.

the negative slopes in an Arrhenius-like pressure plot for $k_{\rm fold}$ indicating a differential decrease in transition state free volume $(\Delta\Delta V^\ddagger_{\rm fold}<0)$ as a function of added Mn²+. On the other hand, the corresponding Arrhenius slopes in Figure 6B for the unfolding rate constants reveal no systematic response to Mn²+ concentration, indicating an approximately constant $\Delta\Delta V^\ddagger_{\rm unfold}$ independent of Mn²+ over 0–50 μ M. To further quantify the Mn²+ effects on pressure-dependent response of the riboswitch, the folding/unfolding activation volumes $(\Delta V^\ddagger_{\rm fold/unfold})$ calculated by eq 2 are summarized in Table 1, to which we will return as an important point of discussion in Section IV.

IIIC. Mg²⁺ Effects on the Pressure-Dependent Riboswitch Folding. The manganese riboswitch has two cationic binding sites, one of which can bind with Mg²⁺ at physiological levels (2 mM) and another that exclusively responds to Mn²⁺ but with a much reduced affinity for Mg²⁺. However, it has also been shown in previous single molecule studies that Mg²⁺ can promote manganese riboswitch folding with or without the cognate ligand. As a parallel thrust, therefore, we have also explored Mg²⁺ and pressure-dependent manganese riboswitch folding to compare the effects of

cognate ligand (Mn^{2+}) vs divalent cation (Mg^{2+}) under nearphysiological concentrations. As illustrated in the pressure van't Hoff plot in Figure 7, the presence of Mg^{2+} at constant

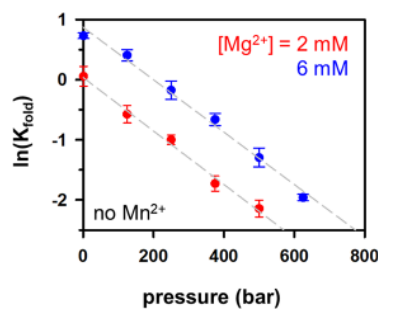


Figure 7. Pressure-dependent equilibrium constant (K_{fold}) data for Mn^{2+} -independent folding of the riboswitch at $[\text{Mg}^{2+}] = 2 \text{ mM}$ (red) and 6 mM (blue).

Mn²⁺ also enhances the equilibrium stability for riboswitch folding, though requiring 1000-fold higher (i.e., mM vs μ M) concentrations. Interestingly, however, the slope of this van't Hoff plot remains constant over an additional 4000 μ M increase in Mg²⁺ concentration, consistent with changes in free volume being insensitive to divalent Mg²⁺ ($\Delta\Delta V^0 \approx 0$). This contrasts with the unambiguously strong effects of Mn²⁺ on pressure-dependent denaturation, confirming that riboswitch folding contributions to $\Delta V^0 > 0$ are clearly both site- and cation-dependent.

Similarly, we can also deconstruct these effects by pressure-dependent investigation of the folding/unfolding kinetics. As illustrated in Figure 8, Mg²⁺-induced folding of the riboswitch is clearly promoted at all pressures. It is interesting to note,

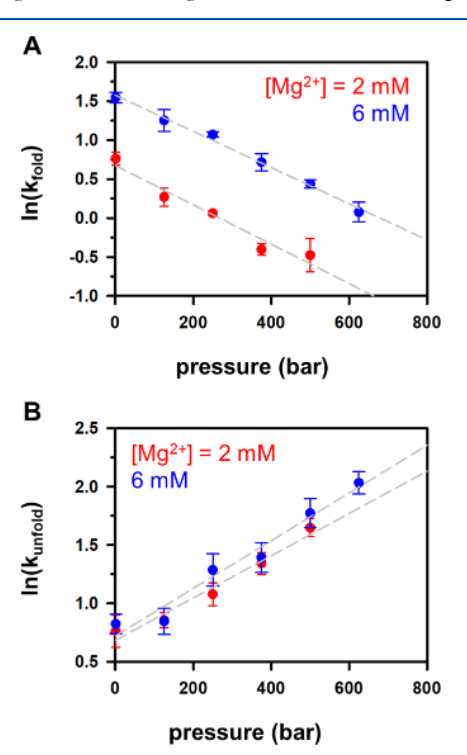


Figure 8. Pressure-dependent analysis of the kinetic rate constants for $\mathrm{Mn^{2+}}$ independent folding of the riboswitch: (A) k_{fold} and (B) k_{unfold} at $\mathrm{[Mg^{2+}]} = 2 \mathrm{\ mM}$ (red) and 6 mM (blue).

however, that such an effect occurs specifically by a ${\rm Mg^{2^+}}$ -dependent increase in $k_{\rm fold}$, with $k_{\rm unfold}$ remaining mostly unchanged—a trend entirely consistent with ${\rm Mg^{2^+}}$ effects found previously at ambient pressures. 30,34 Similar to the trends reported above for equilibrium stabilities ($K_{\rm fold}$), a 4000 $\mu{\rm M}$ increase in ${\rm Mg^{2^+}}$ has no effect on slopes in Figure 8, indicating no significant ${\rm Mg^{2^+}}$ impacts on the transition state activation volumes from either the folding or unfolding direction ($\Delta V^{\ddagger}_{\rm fold}$ and $\Delta V^{\ddagger}_{\rm unfold}$). Simply summarized, manganese riboswitch folding responds to much lower concentrations of the cognate ligand ${\rm Mn^{2^+}}$, with free volume changes (ΔV^0 and $\Delta V^{\ddagger}_{\rm fold}$) decreasing significantly with ${\rm Mn^{2^+}}$ but insensitive to ${\rm Mg^{2^+}}$. As a result, one concludes that ${\rm Mn^{2^+}}$ effects on ΔV^0 and $\Delta V^{\ddagger}_{\rm fold}$ result primarily from highly specific associations of the riboswitch with the cognate ligand as opposed to important but more generic divalent cation effects with ${\rm Mg^{2^+}}$.

IV. DISCUSSION

IVA. Mn²⁺ Association Reduces the Effective Volume of the Riboswitch System. The impact of Mn²⁺ on reducing both ΔV^0 and $\Delta V^{\ddagger}_{\text{fold}}$ has been demonstrated in Section IIIB and shown to be a result of specific cognate ligand effects in Section IIIC. Moreover, the Mn²⁺ effects on the free volume changes are most efficient at low concentration and gradually saturate with increasing concentration (see Table 1). These features are reminiscent of noncooperative binding of Mn²⁺ to the riboswitch, as characterized extensively in previous works. 30,34 Specifically, the riboswitch folding equilibrium constant as a function of Mn²⁺ is well described by a Hill equation with apparent dissociation constant $K_D = 16(5) \mu M$ and near-unity Hill coefficient of n = 1.0(3). This observation motivates an intriguing analysis by which we use these Hill parameters to convert Mn2+ concentration to the fractional occupation (f = 0.0-1.0) of the riboswitch by Mn²⁺, which in turn allows us to generate free volume changes as a function of occupation and as illustrated in Figure 9. Interestingly, while ΔV^0 and $\Delta V^{\ddagger}_{\rm fold}$ exhibit a pronounced linear decrease as a function of ${\rm Mn}^{2+}$ binding, $\Delta V^{\ddagger}_{\rm unfold}$ remains approximately constant throughout the range of Mn2+ concentrations explored. Clearly, any Mn2+ dependence in the overall free

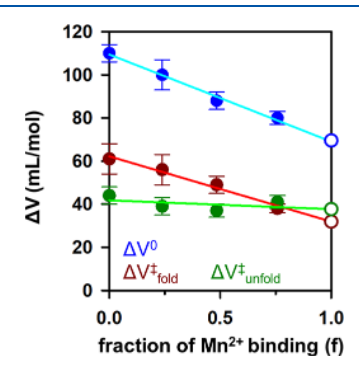


Figure 9. Free volume changes (ΔV^0 and $\Delta V^{\ddagger}_{\rm fold/unfold}$) along the riboswitch folding coordinate, but plotted as a function of fractional binding of ${\rm Mn}^{2+}$ (f=0.0-1.0). The fraction of ${\rm Mn}^{2+}$ -bound riboswitch is calculated from the ${\rm Mn}^{2+}$ concentrations, based on dissociation constant ($K_{\rm D}=16(5)~\mu{\rm M}$) and Hill coefficient (n=1.0(3)) obtained from previous analysis for ${\rm Mn}^{2+}$ -promoted folding of the manganese riboswitch. The open circles represent the predicted volume changes from linear extrapolation to f=1.0.

volume change (ΔV^0) must be attributed to differential changes in volume between the unfolded and transition state conformations $(\Delta V^{\ddagger}_{\rm fold})$, with Mn²⁺ association occurring predominantly prior to the transition state barrier.

Furthermore, the linear dependence of ΔV^0 on ligand binding fraction f allows us to estimate $\Delta V^0 = 69(2)$ mL/mol for folding of the fully Mn²⁺-bound riboswitch by simple extrapolation to f = 1.0. Because the free volume change ΔV^0 for manganese riboswitch folding in the absence of Mn²⁺ is known to be 110(4) mL/mol, we thus infer a large negative change in free volume for Mn2+ binding to the riboswitch $(\Delta V_{\rm bind}^0 \approx -41(4) \text{ mL/mol})$, i.e., approximately 40% and competitive with the overall ΔV^0 for riboswitch folding. Thus, one must conclude that Mn²⁺ association has a considerable effect on the hydration structure of the binding site.^{38–40} Additionally, even though the manganese riboswitch is destabilized with increasing pressure ($\Delta V^0 > 0$), association of the cognate ligand/Mn²⁺ is favored by pressure increase $(\Delta V_{\rm bind}^0 < 0)$, which in turn can compete directly with pressure-dependent denaturation effects on overall RNA folding. One possibility is that such a Mn²⁺-dependent reduction in free volume is due to ligand filling in "voids" formed by the folded riboswitch¹³ or ion recruitment of a more compact water structure in replacement of loosely packed water molecules inside the confined binding pocket. 41 Although more data will be needed to deconstruct pressuredependent ligand binding from biomolecular folding behaviors, the favorable pressure response to ligand association may prove to be a universal feature of riboswitches as well as other ligand-responsive biomolecules. This Mn2+ binding-induced reduction in volume ($\Delta V^0_{\rm bind} < 0$) is significant and may be essential to maintain ligand affinity as well as biochemical function for a riboswitch under pressure.

By way of specific example, the thermophilic bacterium T. maritima is found in the vicinity of hydrothermal vents at the bottom of the ocean. 42 To adapt to such a high-pressure and -temperature environment, the aptamer domain of the T. maritima lysine riboswitch has evolved to contain significantly more GC interactions (38 vs 26 total GC pairs) than its B. subtilis counterpart 43,44 operating in a more ambient pressure/ temperature range.³⁵ In clear contrast, however, the sequences in the aptamer binding sites themselves remain highly conserved between these two versions of the lysine riboswitch.⁴⁵ It therefore makes sense that binding between the lysine ligand and aptamer region might be enhanced $(\Delta V^0_{\rm bind} < 0)$ rather than weakened by pressure destabilization, which in turn would help maintain appropriate riboswitch conformation and biochemical function under high-pressure conditions.

IVB. Insight from Free Volume Changes along the Riboswitch Folding Coordinate. To summarize the volumetric changes associated with manganese riboswitch folding, we have plotted in Figure 10 the differential free volumes (ΔV) for each of the unfolded (U), transition (TS), and folded (F) states. Even more instructively, these ΔV values are each displayed for a series of three Mn²⁺ occupation numbers (f=0, 0.5, and 1.0), with values for the fully ligand-bound riboswitch obtained from linear extrapolation (see Figure 9) to f=1 and all free volumes referenced to zero for the unfolded (U) conformation. From Figure 10, free volume changes for the manganese riboswitch increase monotonically with respect to the folding coordinate, i.e., $V_{\rm U} < V_{\rm TS} < V_{\rm F}$. Specifically, such "staircase" structure confirms a sequential

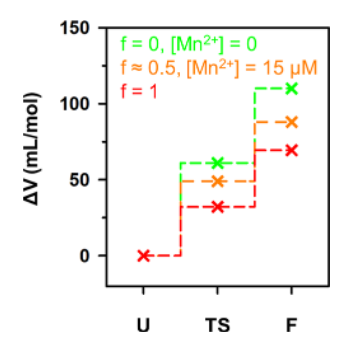


Figure 10. Plot of differential free volume changes (ΔV) along the riboswitch folding coordinate for a variety of $\mathrm{Mn^{2+}}$ conditions, with "staircase-like" structures clearly indicating a monotonic increase in volume at each folding stage. Especially noteworthy is the color-coded parsing of these volume changes with respect to $\mathrm{Mn^{2+}}$ binding fraction, which reveal that >50% of this increase in riboswitch volume is achieved by the time the transition state is formed. Differential volumes are referenced to the unfolded state U at each f.

increase in manganese riboswitch free volume as it folds. Furthermore, such structure is clearly responsible for the simultaneous increase (and decrease) in $k_{\rm unfold}$ (and $k_{\rm fold}$) as a function of applied hydrostatic pressure, respectively, as reported in Section IIIA.

Of particular relevance, however, is the fact that the free volume increase upon folding $(\Delta V^0 > 0)$ diminishes significantly ($\Delta V_{\text{bind}}^0 < 0$) as a function of additional Mn²⁺, which necessarily implies that binding of Mn²⁺ to the aptamer domain decreases the overall riboswitch system volume. As mentioned above, such effects suggest that the cognate ligand replaces a less compact water network in the binding site of the manganese riboswitch.⁴¹ More quantitatively, the magnitudes of the Mn²⁺-dependent staircase "steps" in Figure 10 indicate that >50% of this "shrinkage" is already achieved by the transition state barrier and thus dominated by regions of folding coordinate space where the riboswitch is less structured. By way of confirmation, crystallographic data for the Mn²⁺-bound riboswitch binding pocket reveal that the majority of phosphate ions octahedrally coordinated with Mn²⁺ (including the Mn²⁺-selective nitrogen in A41) arise from nucleotides in the P3 bulge (Figure 1A).³³ From this perspective, it is not surprising that Mn²⁺ would bind to P3 prior to subsequent folding of the riboswitch, for which any loop-loop tertiary interactions between P1 and P3 stems are still largely unformed. Indeed, previous single molecule kinetic studies at $Mg^{2+} \approx 0$ explicitly reveal the folding rate constant to vanish at $Mn^{2+} \approx 0$. Stated alternatively, this implies that Mn^{2+} promotes folding of the manganese riboswitch through an induced fit (IF) "bind-then-fold" mechanism, 30 consistent with the binding/folding pathway postulated above and observed in this work.

As a more subtle observation, however, previous single molecule kinetic studies also provided evidence for a Mg²⁺-promoted switch from an induced fit (IF) to a conformational selection (CS) "fold-then-bind" riboswitch folding mechanism.^{30,34} Specifically, addition of Mg²⁺ at physiological levels (2 mM) allows Mn²⁺ to bind with a 7-fold higher affinity, which was attributed to "preorganization" of the P3 bulge structure prior to tertiary folding of the P1 and P3 domains, i.e., consistent with a conformational selection (CS) "fold-then-bind" pathway. Interestingly, for such an alternative CS pathway, binding of the Mn²⁺ ligand might be expected to

occur in later stages of folding,³¹ which would seem to contradict the results in the paragraph above. By way of resolution, however, we note that IF and CS folding pathways are no longer mutually exclusive in the presence of Mg²⁺. 47,48 Indeed, these kinetic studies could not rule out parallel contributions from an IF "bind-then-fold" folding pathway³⁰ but simply revealed that kinetics of riboswitch folding in the presence of Mg²⁺ to be insensitive to prebinding of Mn²⁺. Specifically, the previous kinetic investigation of k_{unfold} in the presence of Mg²⁺ revealed riboswitch unfolding to occur from both Mn^{2+} -bound (f = 1) and Mn^{2+} -free (f = 0) folded conformations, with the latter now completely consistent with a parallel CS mechanism. 30,49 By way of confirmation, one would expect the Mn2+ binding step required for an IF folding mechanism to primarily impact the free energy landscape region between the unfolded and the transition states, as indeed evident in Figure 10. Simply summarized, pressuredependent characterization of free volume changes complements and extends the previous work by identifying the presence of an additional IF bind-then-fold pathway for riboswitch folding in the presence of Mg²⁺. In conjunction with demonstration in these studies of remarkable sensitivity to cation association and change in hydration, ^{29,36,50,51} such highpressure characterization studies at the single molecule level (and particularly pressure-dependent single molecule kinetics) look well poised to improve our understanding of complex folding mechanisms by providing new and complementary information via "reversible work" $P\Delta V$ free energy surfaces.

V. SUMMARY AND CONCLUSIONS

In this work, we have demonstrated the ability to couple single molecule FRET kinetic measurements with tunable highpressure capillary cell conditions to obtain detailed characterization of free volumes for folding of the manganese riboswitch. On the basis of direct measurement of the pressure-dependent folding/unfolding rate constants, the pressure-induced denaturation of the riboswitch has been unambiguously shown to arise from a simultaneous decrease (increase) in k_{fold} (k_{unfold}), respectively, as a function of increasing pressure and furthermore signaling a sequential, monotonic increase in free volume for the manganese riboswitch along folding coordinate ($V_{\rm U}$ < $V_{\rm TS}$ < $V_{\rm F}$). Moreover, a series of pressure-dependent studies indicate that increase in the cognate ligand Mn²⁺ lowers this free volume change upon folding (i.e., "shrinks" the riboswitch, $\Delta V_{\rm bind}^0$ < 0), particularly between unfolded and transition state conformations. Such a negative change in free volume ($\Delta V_{\rm bind}^0$ < 0) necessarily implies pressure-promoted binding of the cognate ligand, which would compete with pressure-induced destabilization of riboswitch folding ($\Delta V^0 > 0$) and in turn may help mitigate pressure-induced denaturation effects in the biology of deep-sea microorganisms. The study provides a novel reversible work "volumetric" characterization of the free energy folding landscape along riboswitch folding coordinate, which highlights the significance of pre-transition-state effects due to Mn²⁺. Finally, these new volumetric data provide information complementary to our previous kinetic analysis studies under ambient pressure conditions, indicating the parallel presence of both induced fit ("bind-then-fold") and conformational selection ("fold-then-bind") components for folding of the manganese riboswitch.

AUTHOR INFORMATION

Corresponding Author

David J. Nesbitt — JILA, National Institute of Standards and Technology and University of Colorado, Boulder, Colorado 80309, United States; Department of Chemistry and Department of Physics, University of Colorado, Boulder, Colorado 80309, United States; ◎ orcid.org/0000-0001-5365-1120; Email: djn@jila.colorado.edu

Author

Hsuan-Lei Sung – JILA, National Institute of Standards and Technology and University of Colorado, Boulder, Colorado 80309, United States; Department of Chemistry, University of Colorado, Boulder, Colorado 80309, United States

Complete contact information is available at: https://pubs.acs.org/10.1021/acs.jpcb.2c06579

Notes

The authors declare no competing financial interest.

ACKNOWLEDGMENTS

Initial support for this work has been through the National Science Foundation under Grant CHE 1665271/2053117 from the Chemical, Structure, Dynamics and Mechanisms-A Program, with recent transition support from the Air Force Office of Scientific Research (FA9550-15-1-0090) and additional funds for development of the confocal apparatus from PHY-1734006 (Physics Frontier Center Program). We acknowledge early seed contributions by the W. M. Keck Foundation Initiative in RNA Sciences at the University of Colorado, Boulder.

■ REFERENCES

- (1) Heremans, K.; Smeller, L. Protein Structure and Dynamics at High Pressure. *Biochim. Biophys. Acta, Protein Struct. Mol. Enzymol.* **1998**, 1386 (2), 353–370.
- (2) Mitra, L.; Rouget, J.-B.; Garcia-Moreno, B.; Royer, C. A.; Winter, R. Towards a Quantitative Understanding of Protein Hydration and Volumetric Properties. *ChemPhysChem* **2008**, *9* (18), 2715–2721.
- (3) Mozhaev, V. V.; Heremans, K.; Frank, J.; Masson, P.; Balny, C. High Pressure Effects on Protein Structure and Function. *Proteins* **1996**, 24 (1), 81–91.
- (4) Aristides Yayanos, A. Deep-Sea Piezophilic Bacteria. In *Methods in Microbiology*; Academic Press: 2001; Vol. 30, pp 615–637.
- (5) Gross, M.; Jaenicke, R. Proteins under Pressure. Eur. J. Chem. 1994, 221 (2), 617-630.
- (6) Li, L.; Kato, C.; Horikoshi, K. Bacterial Diversity in Deep-Sea Sediments from Different Depths. *Biodivers. Conserv.* **1999**, 8 (5), 659–677.
- (7) Jannasch, H. W.; Wirsen, C. O. Variability of Pressure Adaptation in Deep sea Bacteria. *Arch. Microbiol.* **1984**, *139* (4), 281–288.
- (8) Najaf-Zadeh, R.; Wu, J. Q.; Macgregor, R. B. Effect of Cations on the Volume of the Helix-Coil Transition of Poly[d(A-T)]. *Biochim. Biophys. Acta* •ene Regul. 1995, 1262 (1), 52–58.
- (9) Lin, M.-C.; Macgregor, R. B. Activation Volume of DNA Duplex Formation. *Biochemistry* **1997**, *36* (21), 6539–6544.
- (10) Downey, C. D.; Crisman, R. L.; Randolph, T. W.; Pardi, A. Influence of Hydrostatic Pressure and Cosolutes on RNA Tertiary Structure. J. Am. Chem. Soc. 2007, 129 (30), 9290–9291.
- (11) Patra, S.; Anders, C.; Schummel, P. H.; Winter, R. Antagonistic Effects of Natural Osmolyte Mixtures and Hydrostatic Pressure on the Conformational Dynamics of a DNA Hairpin Probed at the Single-Molecule Level. *Phys. Chem. Chem. Phys.* **2018**, 20 (19), 13159–13170.

- (12) Ramanujam, V.; Alderson, T. R.; Pritišanac, I.; Ying, J.; Bax, A. Protein Structural Changes Characterized by High-Pressure, Pulsed Field Gradient Diffusion NMR Spectroscopy. *J. Magn. Reson.* **2020**, 312, 106701.
- (13) Frye, K. J.; Royer, C. A. Probing the Contribution of Internal Cavities to the Volume Change of Protein Unfolding Under Pressure. *Protein Sci.* **1998**, 7 (10), 2217–2222.
- (14) Cioni, P. Role of Protein Cavities on Unfolding Volume Change and on Internal Dynamics under Pressure. *Biophys. J.* **2006**, *91* (9), 3390–3396.
- (15) Roche, J.; Caro, J. A.; Norberto, D. R.; Barthe, P.; Roumestand, C.; Schlessman, J. L.; Garcia, A. E.; García-Moreno, E. B.; Royer, C. A. Cavities Determine the Pressure Unfolding of Proteins. *Proc. Natl. Acad. Sci. U. S. A.* **2012**, *109* (18), 6945–6950.
- (16) Grigera, J. R.; McCarthy, A. N. The Behavior of the Hydrophobic Effect under Pressure and Protein Denaturation. *Biophys. J.* **2010**, 98 (8), 1626–1631.
- (17) Royer, C.; Winter, R. Protein Hydration and Volumetric Properties. Curr. Opin. Colloid Interface Sci. 2011, 16 (6), 568–571.
- (18) Nucci, N. V.; Fuglestad, B.; Athanasoula, E. A.; Wand, A. J. Role of Cavities and Hydration in the Pressure Unfolding of T₄ Lysozyme. *Proc. Natl. Acad. Sci. U. S. A.* **2014**, *111* (38), 13846–13851.
- (19) Hillson, N.; Onuchic, J. N.; García, A. E. Pressure-Induced Protein-Folding/Unfolding Kinetics. *Proc. Natl. Acad. Sci. U. S. A.* **1999**, 96 (26), 14848–14853.
- (20) Woenckhaus, J.; Köhling, R.; Winter, R.; Thiyagarajan, P.; Finet, S. High Pressure-Jump Apparatus for Kinetic Studies of Protein Folding Reactions Using the Small-Angle Synchrotron X-Ray Scattering Technique. *Rev. Sci. Instrum.* **2000**, *71* (10), 3895–3899.
- (21) Nguyen, L. M.; Roche, J. High-Pressure NMR Techniques for the Study of Protein Dynamics, Folding and Aggregation. *J. Magn. Reson.* **2017**, 277, 179–185.
- (22) Mustoe, A. M.; Brooks, C. L.; Al-Hashimi, H. M. Hierarchy of RNA Functional Dynamics. *Annu. Rev. Biochem.* **2014**, 83 (1), 441–466.
- (23) Al-Hashimi, H. M.; Walter, N. G. RNA Dynamics: it is About Time. Curr. Opin. Struct. Biol. 2008, 18 (3), 321–329.
- (24) Lai, D.; Proctor, J. R.; Meyer, I. M. On the Importance of Cotranscriptional RNA Structure Formation. *RNA* **2013**, *19* (11), 1461–1473.
- (25) Schärfen, L.; Neugebauer, K. M. Transcription Regulation Through Nascent RNA Folding. J. Mol. Biol. 2021, 433 (14), 166975.
- (26) Schneider, S.; Paulsen, H.; Reiter, K. C.; Hinze, E.; Schiene-Fischer, C.; Hübner, C. G. Single Molecule FRET Investigation of Pressure-Driven Unfolding of Cold Shock Protein A. J. Chem. Phys. **2018**, *148* (12), 123336.
- (27) Sung, H.-L.; Nesbitt, D. J. DNA Hairpin Hybridization under Extreme Pressures: A Single-Molecule FRET Study. *J. Phys. Chem. B* **2020**, *124* (1), 110–120.
- (28) Hodak, J. H.; Fiore, J. L.; Nesbitt, D. J.; Downey, C. D.; Pardi, A. Docking Kinetics and Equilibrium of a GAAA Tetraloop-Receptor Motif Probed by Single-Molecule FRET. *Proc. Natl. Acad. Sci. U. S. A.* **2005**, *102* (30), 10505–10510.
- (29) Sung, H.-L.; Nesbitt, D. J. Single-Molecule Kinetic Studies of DNA Hybridization under Extreme Pressures. *Phys. Chem. Chem. Phys.* **2020**, 22 (41), 23491–23501.
- (30) Sung, H.-L.; Nesbitt, D. J. Single-Molecule FRET Kinetics of the Mn²⁺ Riboswitch: Evidence for Allosteric Mg²⁺ Control of "Induced-Fit" vs "Conformational Selection" Folding Pathways. *J. Phys. Chem. B* **2019**, *123* (9), 2005–2015.
- (31) Suddala, K. C.; Price, I. R.; Dandpat, S. S.; Janeček, M.; Kührová, P.; Šponer, J.; Banáš, P.; Ke, A.; Walter, N. G. Local-to-Global Signal Transduction at the Core of a Mn²⁺ Sensing Riboswitch. *Nat. Commun.* **2019**, *10* (1), 4304.
- (32) Dambach, M.; Sandoval, M.; Updegrove, T. B.; Anantharaman, V.; Aravind, L.; Waters, L. S.; Storz, G. The Ubiquitous *yybP-ykoY* Riboswitch is a Manganese-Responsive Regulatory Element. *Mol. Cell* **2015**, *57* (6), 1099–1109.

- (33) Price, I. R.; Gaballa, A.; Ding, F.; Helmann, J. D.; Ke, A. Mn²⁺-Sensing Mechanisms of *yybP-ykoY* Orphan Riboswitches. *Mol. Cell* **2015**, 57 (6), 1110–1123.
- (34) Sung, H.-L.; Nesbitt, D. J. Novel Heat-Promoted Folding Dynamics of the *yybP-ykoY* Manganese Riboswitch: Kinetic and Thermodynamic Studies at the Single-Molecule Level. *J. Phys. Chem. B* **2019**, *123* (26), 5412–5422.
- (35) Aitken, C. E.; Marshall, R. A.; Puglisi, J. D. An Oxygen Scavenging System for Improvement of Dye Stability in Single-Molecule Fluorescence Experiments. *Biophys. J.* **2008**, *94* (5), 1826–1835
- (36) Sung, H.-L.; Nesbitt, D. J. High Pressure Single-Molecule FRET Studies of the Lysine Riboswitch: Cationic and Osmolytic Effects on Pressure Induced Denaturation. *Phys. Chem. Chem. Phys.* **2020**, 22 (28), 15853–15866.
- (37) Sung, H.-L.; Nesbitt, D. J. Sequential Folding of the Nickel/Cobalt Riboswitch Is Facilitated by a Conformational Intermediate: Insights from Single-Molecule Kinetics and Thermodynamics. *J. Phys. Chem. B* **2020**, 124 (34), 7348–7360.
- (38) Sun, L.-Z.; Chen, S.-J. Predicting RNA-Metal Ion Binding with Ion Dehydration Effects. *Biophys. J.* **2019**, *116* (2), 184–195.
- (39) Ma, C. Y.; Pezzotti, S.; Schwaab, G.; Gebala, M.; Herschlag, D.; Havenith, M. Cation Enrichment in the Ion Atmosphere is Promoted by Local Hydration of DNA. *Phys. Chem. Chem. Phys.* **2021**, 23 (40), 23203–23213.
- (40) Draper, D. E. RNA Folding: Thermodynamic and Molecular Descriptions of the Roles of Ions. *Biophys. J.* **2008**, 95 (12), 5489–5495
- (41) Knight, A. W.; Kalugin, N. G.; Coker, E.; Ilgen, A. G. Water Properties under Nano-Scale Confinement. *Sci. Rep.* **2019**, 9 (1), 8246.
- (42) Serganov, A.; Huang, L.; Patel, D. J. Structural Insights into Amino Acid Binding and Gene Control by a Lysine Riboswitch. *Nature* **2008**, 455 (7217), 1263–1267.
- (43) Garst, A. D.; Héroux, A.; Rambo, R. P.; Batey, R. T. Crystal Structure of the Lysine Riboswitch Regulatory mRNA Element. *J. Biol. Chem.* **2008**, 283 (33), 22347–22351.
- (44) Blouin, S.; Lafontaine, D. A. A Loop—Loop Interaction and a K-Turn Motif Located in the Lysine Aptamer Domain are Important for the Riboswitch Gene Regulation Control. *RNA* **2007**, *13* (8), 1256—1267.
- (45) Serganov, A.; Patel, D. J. Amino Acid Recognition and Gene Regulation by Riboswitches. *Biochim. Biophys. Acta* ◆*ene Regul. Mech.* 2009, 1789 (9), 592–611.
- (46) Vogt, A. D.; Di Cera, E. Conformational Selection or Induced Fit? A Critical Appraisal of the Kinetic Mechanism. *Biochemistry* **2012**, *51* (30), 5894–5902.
- (47) Pavlović, R. Z.; Lalisse, R. F.; Hansen, A. L.; Waudby, C. A.; Lei, Z.; Güney, M.; Wang, X.; Hadad, C. M.; Badjić, J. D. From Selection to Instruction and Back: Competing Conformational Selection and Induced Fit Pathways in Abiotic Hosts. *Angew. Chem.* **2021**, *60* (36), 19942–19948.
- (48) Hammes, G. G.; Chang, Y.-C.; Oas, T. G. Conformational Selection or Induced Fit: A Flux Description of Reaction Mechanism. *Proc. Natl. Acad. Sci. U. S. A.* **2009**, *106* (33), 13737–13741.
- (49) Suddala, K. C.; Wang, J.; Hou, Q.; Walter, N. G. Mg²⁺ Shifts Ligand-Mediated Folding of a Riboswitch from Induced-Fit to Conformational Selection. *J. Am. Chem. Soc.* **2015**, 137 (44), 14075–14083.
- (50) Fan, H. Y.; Shek, Y. L.; Amiri, A.; Dubins, D. N.; Heerklotz, H.; Macgregor, R. B.; Chalikian, T. V. Volumetric Characterization of Sodium-Induced G-Quadruplex Formation. *J. Am. Chem. Soc.* **2011**, 133 (12), 4518–4526.
- (51) Patra, S.; Anders, C.; Erwin, N.; Winter, R. Osmolyte Effects on the Conformational Dynamics of a DNA Hairpin at Ambient and Extreme Environmental Conditions. *Angew. Chem.* **2017**, *56* (18), 5045–5049.

□ Recommended by ACS

Molecular Dynamics Simulation Investigation of the Binding and Interaction of the EphA6–Odin Protein Complex

Jianhua Wu, Ran Jia, et al.

JUNE 22, 2022

THE JOURNAL OF PHYSICAL CHEMISTRY B

READ 🗹

Unraveling the Mechanics of a Repeat-Protein Nanospring: From Folding of Individual Repeats to Fluctuations of the Superhelix

Marie Synakewicz, Johannes Stigler, et al.

MARCH 08, 2022

ACS NANO

READ 🗹

Direct Observation of the Mechanical Role of Bacterial Chaperones in Protein Folding

Deep Chaudhuri, Shubhasis Haldar, et al.

JUNE 09, 2022

BIOMACROMOLECULES

READ 🗹

Exploiting a Mechanical Perturbation of a Titin Domain to Identify How Force Field Parameterization Affects Protein Refolding Pathways

David Wang and Piotr E. Marszalek

APRIL 03, 2020

JOURNAL OF CHEMICAL THEORY AND COMPUTATION

READ 🗹

Get More Suggestions >